Title: pH-dependent beta-lactam resistance in *Klebsiella pneumoniae* is mediated by paralogous class B PBPs and the class A PBP, PBP1b.

Authors

Sarah Beagle[1] and Petra Anne Levin[1*]

Affiliations

[1]Washington University in St. Louis, Department of Biology, St. Louis, Missouri, USA

*Correspondence: plevin@wustl.edu

Abstract

Klebsiella pneumoniae is a leading cause of global deaths due to antibiotic resistance. Of particular concern, is the rapid expansion of resistance to beta-lactam antibiotics within *K. pneumoniae* lineages. The environmental factors that influence pathogen physiology and, subsequently, antibiotic resistance remain poorly understood. Here we demonstrate that physiologically-relevant reductions in pH increased antibiotic resistance as much as 64-fold, with the most dramatic increases observed for beta-lactams that inhibit cell division. We identified two genes that contribute to acid-dependent beta-lactam resistance, the class A PBP, PBP1b, and the paralogous class B PBP, $PBP3_{PARA}$. Loss of either gene increases *K. pneumoniae* susceptibility to beta-lactams at low pH. Our data supports previous work from our group and others indicating that functional redundancy among cell wall synthesis enzymes allows for specialization and ensures robust cell wall synthesis across a range of environmental conditions.

Introduction

The cell wall or peptidoglycan (PG) is an essential structure that provides shape and structural rigidity to bacterial cells. PG is comprised of glycan strands of repeating linked N-acetylglucosamine (NAG) and N-acetylmuramic acid (NAM) sugars that are crosslinked together by short peptide chains [1]. Synthesis and maintenance of PG requires many enzymatic steps that occur across multiple cellular locations; PG precursors are built in the cytoplasm, transported through the inner membrane, and fully assembled into PG within the periplasmic space. Within members of *Enterobacteriaceae* the process of periplasmic PG assembly is highly enzymatically redundant, with approximately four enzymes capable of carrying out a single periplasmic PG

synthesis reaction. This apparent functional redundancy is particularly striking when compared to the earlier cytoplasmic PG synthesis reactions, which occur in a nearly 1:1 enzyme-to-reaction ratio[2]. While cell wall precursors are assembled in the relatively protected cytoplasm, the wall itself is built in the periplasm and thus exposed to the physicochemical environment.

Penicillin-binding proteins (PBPs) carry out essential transpeptidation reactions in the periplasm. Class A PBPs are bi-functional enzymes that both link the NAG-NAM sugar moieties together (transglycosylation, TG) as well as crosslink the peptide stems of adjacent glycan strands (transpeptidation, TP). In *Escherichia coli,* the primary class A PBPs are PBP1a and PBP1b, which are encoded by *mrcA* and *mrcB* respectively. PBP1a and PBP1b are individually dispensable for growth, but loss of both is lethal[3–5]. A third class A PBP, PBP1c (*pbpC*), has an unknown role in PG synthesis and maintenance, as loss of this gene does not result in discernable defects under standard laboratory conditions[6]. Class B PBPs are monofunctional transpeptidases; these PBPs work in conjunction with cognate glycosyltransferases. PBP2 and PBP3 are the canonical class B PBPs in Gram-negative bacteria, and they function within the elongation and division machinery respectively.

The essentiality of the bacterial cell wall renders the enzymes that synthesize PG attractive drug targets. Beta-lactams, the most prescribed cell-wall-targeting class of antibiotics, interfere with PG synthesis by irreversibly binding to the transpeptidase domain of PBPs and inhibiting transpeptidation[7]. Work done in *Escherichia coli* demonstrated that resistance to Beta-lactam varies across physiochemical conditions. Specifically, *E. coli* exhibits increased resistance to PBP2- and PBP3-targeting Beta-lactams when cells are grown in mildly acidic pH conditions (~pH 5). Growth at low pH as well as acid-dependent Beta-lactam resistance required the Class A PBP, PBP1b, while full fitness during growth in alkaline pH required PBP1a[8]. These results indicate that the apparent functional redundancy in PG synthesis enzymes allows for specialization of enzymes, thereby ensuring that cell wall synthesis is robust across a wide range of environmental conditions. To determine if this response is conserved in a pathogen, we assessed the impact of environmental pH on Beta-lactam resistance in *Klebsiella pneumoniae,* a Gram-negative, encapsulated, opportunistic human pathogen.

Infections caused by *K. pneumoniae,* a close relative of *E. coli,* are increasingly difficult to treat due to dramatic rises in antibiotic resistance. *K. pneumoniae* is a dominant member of two different Beta-lactam-resistant groups of bacteria, Extended-spectrum-Beta-lactamase (ESBL)-

60 producing *Enterobacteriaceae* and Carbapenem-resistant *Enterobacteriaceae* (CRE) that have
61 been labeled serious and urgent public health threats by the CDC[9]. In 2019, *K. pneumoniae* was the
62 third leading cause of global deaths where the death was directly due to or associated with
63 antibiotic resistance[10], highlighting the need to explore how environmental factors impact
64 pathogen physiology and subsequently, antibiotic resistance.

65 Here we evaluated the impact of pH on *K. pneumoniae* response to beta-lactams and found that
66 resistance increased as much as 64-fold during growth in mildly acidic conditions. Genetic
67 analysis identified two cell wall synthesis genes, *mrcB* and *ftsI2* that are critical for pH-dependent
68 changes in antibiotic resistance. *mrcB* encodes PBP1b, a bifunctional class A PBP we previously
69 identified as a contributor to pH-dependent antibiotic resistance in *E. coli*[8]. Induced at low pH,
70 *ftsZ2* encodes $PBP3_{PARA,}$ a paralogous copy of the canonical, division-associated class B PBP,
71 PBP3. $PBP3_{PARA}$ is required for both acid-dependent beta-lactam resistance and robust growth and
72 division at low pH, highlighting the fitness advantage conferred by functional redundancy amongst
73 bacterial PBPs. **Results**

74 ***Klebsiella pneumoniae* exhibits acid-dependent resistance to Beta-lactam antibiotics.**

75 To determine the impact of pH on *K. pneumoniae* beta-lactam susceptibility, we assessed the
76 response of a urinary tract infection (UTI) isolate, *K. pneumoniae* TOP52[11] to a panel of beta-
77 lactams during growth across a range of physiologically relevant pH conditions. The drug panel
78 included beta-lactams that preferentially target PBPs in the divisome (i.e. Cephalexin, Aztreonam,
79 and Piperacillin) or the elongasome (Meropenem, Doripenem), as well as non-specific inhibitors
80 (Ampicillin, Carbenicillin) that have similar affinities for all PBPs[12]. Relative susceptibility or
81 resistance to a given Beta-lactam was determined by comparing the minimal inhibitory
82 concentration of drug at neutral pH to that at other pH values.

83 *K. pneumoniae* exhibited a 2-64-fold increase in resistance to the entire spectrum of tested beta-
84 lactams at pH values < 5 relative to resistance at pH 7. (Fig 1A, Sup Table 3). We observed strong
85 acid-dependent increases in resistance for drugs that preferentially target PBP3, with Aztreonam
86 (AZT) and Cephalexin (CEX) MICs increasing as much as 20- and 64-fold respectively at pH 4.8.
87 Resistance to PBP2-targeting Beta-lactams increased modestly at low pH, with MICs to Doripenem
88 (DOR) and Meropenem (MER) increasing 2- to 4-fold. In contrast to *E. coli*[8], we also observed a

89 modest 2- to 4-fold increases in resistance to the non-specific Beta-lactams, Ampicillin (AMP) and
90 Carbenicillin (CAR) at low pH.

91 Low pH not only enabled growth at concentrations of drug that are lethal at neutral pH but also
92 preserved cell morphology (Fig 1 C & D). Consistent with increased intrinsic resistance at low pH,
93 the characteristic rod-shaped morphology of *K. pneumoniae* was preserved during growth under
94 acidic conditions in concentrations of Beta-lactams that cause either cell rounding (Meropenem)
95 or filamentation (Cephalexin) at neutral pH. The observed acid-dependent increased resistance to
96 beta-lactams is not strain specific behavior as *K. pneumoniae* strains NTUH-K2044 and ATCC
97 43816 also exhibit a 4-fold increase to Meropenem (MER) and an ~32-fold increase to Cephalexin
98 (CEX) when grown at pH 4.8 versus pH 6.8 (Fig. 1B). Together, these data suggest that acid-
99 dependent beta-lactam resistance is a conserved response within *K. pneumoniae*.

100 **Acid-dependent Beta-lactam resistance is independent of endogenous beta-lactamase**
101 **expression.**

102 *K. pneumoniae* encodes an endogenous class-A beta-lactamase, bla_{SHV-1}, which confers increased
103 resistance to the Penicillin subclass of Beta-lactams[7,11,13]. To determine if expression of bla_{SHV-1} is
104 influencing the resistance profiles at low pH, we generated a deletion strain (Δbla_{SHV-1}) and
105 repeated the MIC assays under both acidic and neutral pH conditions. We observed increased
106 sensitivity to the Penicillin sub-classes of Beta-lactams tested (AMP, CAR, PIP) in both pH
107 environments (Sup Table 5). Consistent with the specificity of bla_{SHV-1}, loss of bla_{SHV-1} did not alter
108 the MICs to non-Penicillin beta-lactams at either pH (Sup Table 5). However, the Δbla_{SHV-1} mutant
109 still displayed increased resistance to all tested Beta-lactams at low pH relative to neutral pH (Fig 2
110 A-D, Supp table 5), demonstrating that acid-dependent resistance is independent of endogenous
111 beta-lactamase expression.

112 **pH modulates expression of Class B PBP paralogs in *K. pneumoniae*.**

113 To ascertain the impact of pH on expression of genes encoding PBPs or other cell wall synthesis
114 genes, we performed RNAseq in *K. pneumoniae* comparing cells cultured in acidic (pH 4.8) versus
115 neutral pH media (pH 6.8). Consistent with previous studies, pH does not impact expression of
116 class A PBPs, *mrcA* (PBP1a) or *mrcB* (PBP1b), in either *E. coli* or *K. pneumoniae*[14,15] (Table 1) .
117 PBP1c, a cryptic class A PBP with no demonstrated role in cell wall synthesis under standard
118 laboratory conditions, exhibits an ~2-fold decrease in expression during growth in acidic pH. We

observed no significant changes expression of the class B PBPs between pH conditions, but there was an order of magnitude increase in expression at low pH of genes we designated *mrdA2* and *ftsI2*, which encode paralogous copies of class B PBPs, referred to here as $PBP2_{PARA}$ and $PBP3_{PARA}$ (Fig 3 A&B). In addition to the class B paralogs, several other cell wall synthesis genes displayed pH-responsive expression profiles. Most notably, two carboxypeptidases, *dacA* (PBP5) and *dacD* (PBP6b), exhibited modest increases of 2- to 3-fold in expression during growth at low pH. Both *dacA* and *dacD* are implicated in maintaining proper cell morphology in *E. coli*, with *dacD* being required for proper morphology specifically at low pH[16,17].

Loss of $PBP3_{PARA}$ results in filamentation in *K. pneumoniae* at low pH.

Duplications of the class B PBPs, PBP2 and PBP3, have expanded the repertoire of cell wall synthesis enzymes in several pathogens within the *Enterobacteriaceae* family[18–20]. Class B PBP paralogs in *Salmonella enterica* serovar Typhimurium (*S.* Typhimurium) referred to as $PBP2_{SAL}$ and $PBP3_{SAL}$ are thought to be important for maximal fitness during growth at low pH. Expression of both $PBP2_{SAL}$ and $PBP3_{SAL}$ is maximally induced at low pH (<5.8), and loss of $PBP2_{SAL}$ has been reported to impair rod-shape morphology under acidic environments[19,20].

As with $PBP2_{SAL}$ and $PBP3_{SAL}$, $PBP2_{PARA}$ and $PBP3_{PARA}$ share significant sequence identity with their canonical counterparts (59% for $PBP2_{PARA}$ and 61% for $PBP3_{PARA}$) and retain the sequence motifs associated with catalysis, but their contributions to cell wall maintenance in *Klebsiella* is unknown [Fig 3 C&D, Sfig 2]. We generated individual gene deletion strains and examined the mutants using cell size analysis and time-lapse microscopy to evaluate the role of the class B PBP paralogs in cell size and division. We cultured cells at both acidic and neutral pH and sampled cultures at early exponential phase (OD_{600} = 0.1-0.2) for cell size analysis. While loss of $PBP2_{PARA}$ did not impact cell size or morphology at either pH, we found that during growth at pH 4.8 the $PBP3_{PARA}$ deletion mutant exhibited heterogeneous cell lengths, with many cells displaying filamentous behavior indicative of cell division defects (Fig4 A&B, Sfig 2). Using a definition of filamentation as a cell length of >15 μM which represents ~3X the average length of WT cells at pH 4.8 (3.9 ± 0.2 μM, Fig 4B), we determined that 21-58% of $PBP3_{PARA}$ deficient cells within a given population were filamentous, with a smaller proportion of cells (3-17%) reaching lengths of >40 μM. The division defects associated with loss of $PBP3_{PARA}$ were specific to growth in acidic conditions, as growth at neutral pH resulted in an average cell length for the $PBP3_{PARA}$ deficient cells that was consistent with WT cell lengths (Fig 3C).

149 Time-lapse microscopy of acid-grown Δ*ftsI2* cells spotted onto acidic LB agarose pads revealed a
150 population of cells with heterogeneous lengths that displayed clear division defects as cells
151 continued to elongate without successful division resulting in long filamentous cells. Whereas
152 spotting acid-grown Δ*ftsI2* cells onto LB agarose pads at neutral pH restored division to the
153 filamentous cells (Sfig 3). Complementation of *ftsI2* in trans from a medium-copy number plasmid
154 enabled division and restored cell lengths consistent with WT at low pH (Fig 4 A&B). Together these
155 data suggest that the activity of the canonical PBP3 is impaired under acidic conditions and that
156 $PBP3_{PARA}$ is the predominant transpeptidase supporting cell division in *K. pneumoniae* at low pH.

157 **Loss of PBP1b or $PBP3_{PARA}$ differentially impacts Beta-lactam resistance at low pH in *Klebsiella***

158 The increased expression of genes encoding $PBP2_{PARA}$ and $PBP3_{PARA}$ and other cell wall
159 maintenance proteins at low pH raised the possibility that these proteins might contribute to acid-
160 dependent Beta-lactam resistance. To address this hypothesis, we generated strains individually
161 defective in a subset of *K. pneumoniae* genes implicated in cell wall or shape maintenance and
162 assayed their response to beta-lactam antibiotics during growth at acidic and neutral pH
163 conditions. In addition to genes that displayed pH-dependent expression, we also evaluated the
164 role of class A PBPs in *K. pneumoniae* response to beta-lactams across pH conditions. The class A
165 PBPs are known to influence antibiotic response in *E. coli*. While most individual mutations did not
166 significantly impact acid-dependent-Beta-lactam resistance, loss of PBP1b or $PBP3_{PARA}$ altered
167 sensitivities to Beta-lactams at low pH (Fig 2A-D).

168 Loss of PBP1b (Δ*mrcB*) most dramatically affected acid-dependent resistance to Cephalexin. A
169 Δ*mrcB* mutant displayed only a 4-fold increase in cephalexin MIC at low pH versus at neutral pH,
170 while the WT has a 64- to 128-fold increase in resistance under the same conditions. The Δ*mrcB*
171 mutant also no longer exhibited acid-dependent resistance to the generalist (AMP) and PBP2-
172 targeting- (DOR, MER) beta-lactams, (Fig 2 A-D). Defects in PBP1b also led to a nearly 10-fold
173 increase in susceptibility to Cefsulodin in both acidic and neutral pH compared to WT (Sup Table
174 5). The increase in sensitivity at all pHs of the ΔPBP1b mutant is consistent with data suggesting
175 that PBP1a is more sensitive to Cefsulodin[21,22].

176 Loss of $PBP3_{PARA}$ differentially impacted resistance to beta-lactams. The $PBP3_{PARA}$ null mutant no
177 longer displayed acid-dependent resistance to Ampicillin and Cefsulodin at low pH (Fig 2A & B). In
178 fact, a $PBP3_{PARA}$ deletion mutant was more sensitive to Ampicillin at low pH than at neutral pH (Fig

179 2A). When challenged with PBP3-targeting Beta-lactams (CEX, AZT, PIP), the $PBP3_{PARA}$ deletion
180 mutant still retained mild acid-dependent resistance but was 2- to 8-fold more sensitive at low pH
181 than WT (Fig 4 D, 5 B). Surprisingly, the $PBP3_{PARA}$ null mutant exhibited increased resistance when
182 challenged with PBP2-targeting beta-lactams at low pH. The Meropenem and Doripenem MICs
183 obtained for the $PBP3_{PARA}$ null mutant were 12-16-fold higher at acidic pH versus neutral pH. For
184 comparison, WT cells only exhibited a 2-4-fold increase in MIC to these two drugs at acidic pH (Fig
185 4C, 5A). Despite the ~10-fold increases in expression under acidic conditions, loss of *mrdA2,*
186 encoding PBP2, had no significant impact on Beta-lactam susceptibility across pH values.

187 **Increased acid-dependent resistance to PBP2-targeting compounds in the $PBP3_{PARA}$ null**
188 **mutant requires $PBP2_{PARA}$**

189 We reasoned that the unexpected increase to PBP2-inhibitors at low pH observed in the Δ*ftsI2*
190 mutant could be influenced by the presence of $PBP2_{PARA}$. To address this possibility, we generated
191 a double deletion strain lacking both class B paralogs (Δ*ftsI2* Δ*mrdA2*) and assayed its response to
192 beta-lactams with high specificity for PBP2 or PBP3 at both neutral and acidic pH. Deletion of both
193 class B PBP paralogs eliminated the dramatic increase in resistance at low pH (4.8), restoring WT-
194 level responses to both Doripenem and Meropenem. When challenged with PBP3-targeting Beta-
195 lactams, the double mutant class B paralog mutant phenocopied the Δ*ftsI2* mutant, displaying
196 similar reductions in resistance at low pH (Fig 5). Together these data suggest that both $PBP2_{PARA}$
197 and $PBP3_{PARA}$ are involved in mediating resistance to PBP2-inhibitors, whereas resistance to PBP3-
198 targeting Beta-lactams is primarily facilitated by $PBP3_{PARA}$.

199 **Discussion**

200 As observed in *E. coli,* beta-lactam resistance in *K. pneumoniae* increases substantially during
201 growth in acidified medium (Fig 1A).We find that the class A PBP, PBP1b, and the acid-responsive
202 paralogous copy of the class B PBP, $PBP3_{PARA}$, are major genetic contributors to acid-mediated
203 beta-lactam resistance in *K. pneumoniae*. Disruption of *mrcB*, the gene encoding PBP1b,
204 eliminates acid-mediated resistance to the class B PBP inhibitors, Meropenem, Doripenem, and
205 Cephalexin. Loss of $PBP3_{PARA}$ differentially impacts beta-lactam resistance, with mutants showing
206 sensitization towards Ampicillin, Cefsulodin, and all PBP3-targeting beta-lactams but increased
207 resistance towards PBP2-targeting antibiotics.

208 While both *E. coli* and *K. pneumoniae* demonstrate acid-dependent beta-lactam resistance,
209 factors influencing this phenomenon differ between the two organisms. Acid-mediated beta-
210 lactam resistance in *E. coli* appears to be solely due to intrinsic properties of the PBP enzymes,
211 particularly PBP1b[8], while in *K. pneumoniae* the contribution of PBP1b is supplemented by pH-
212 dependent induction of genes encoding paralogous class B PBPs. Although we only observed
213 changes to antibiotic susceptibility in a $PBP3_{PARA}$ null mutant, loss of $PBP2_{PARA}$ impacted the
214 morphological response to PBP2-targeting antibiotics at low pH (Fig 5 C). This result suggests that
215 $PBP2_{PARA}$ plays a role in maintaining PG and cell shape at low pH. Together, our findings support a
216 modular model of cell wall synthesis within the *Enterobacteriaceae* family where apparent function
217 redundancy amongst cell wall synthesis enzymes is protective by enabling PG synthesis across a
218 range of pH conditions.

219 **The Class A PBP, PBP1b, is important for acid-dependent beta-lactam resistance in *K.***
220 ***pneumoniae***

221 PBP1b is required for resistance to PBP2- and PBP3-targeting beta-lactams and for growth at low
222 pH (<5) in *E. coli*[8]. In contrast, deletion of PBP1b in *K. pneumoniae* did not significantly impair
223 growth in acidified culture medium (pH 4.8), suggesting that there are key differences in how PBP1b
224 influences growth in acidic environments between *E. coli* and *K. pneumoniae* (Sfig 4). While
225 expression of *mrcB,* encoding PBP1b, was not influenced by pH, loss of PBP1b impaired *K.*
226 *pneumoniae's* resistance to Ampicillin, Doripenem, Meropenem, and Cephalexin at low pH (Fig 2,
227 Supp Table 5). Consistent with MIC data, a PBP1b-deficient strain exhibits faster killing kinetics
228 than a WT strain in the presence of Cephalexin at low pH (Fig 2 E &F). While filamentation is a
229 characteristic morphology associated with division-targeting beta-lactams[23,24], at low pH a PBP1b-
230 deficient *K. pneumoniae* strain is sensitive to Cephalexin at concentrations that do not elicit
231 filamentation (Fig 4E). The time frame for lysis of the PBP1b mutant is rapid with more than 50% of
232 the population exhibiting signs of membrane integrity as denoted by propidium iodide staining
233 within 90 minutes of exposure to Cephalexin at low pH (Fig 2F).

234 Notably, at neutral pH a *ΔmrcB* mutant did not display significant changes in MIC across beta-
235 lactam classes (Sup Table 5), suggesting that PBP1B specifically mediates beta-lactam resistance
236 at low pH in *K. pneumoniae*. This finding differs from what has been observed in *E. coli* where loss
237 of either PBP1b or its cognate outer membrane activator, LpoB, increases sensitivity to multiple
238 classes of beta-lactams at neutral pH[25,26]. Our data demonstrating that a PBP1b mutant is more

239 sensitive to PBP2- and PBP3-targeting beta-lactams is consistent with prior studies reporting
240 interactions between PBP1b and key division and elongasome proteins[27,2820]. Based on these data,
241 we propose that PBP1b supports cell wall integrity at low pH through interactions with other cell
242 division proteins.

243 **Class B PBP paralogs modulate pH-dependent changes in beta-lactam resistance**

244 Although, low pH induced expression of genes encoding both *K. pneumoniae's* PBP2 and PBP3
245 paralogs (Table 1), only defects in *ftsI2,* encoding $PBP3_{PARA}$, sensitized cells to beta-lactams during
246 growth in acidified medium. Defects in *mrdA2*, encoding $PBP2_{PARA}$, did not significantly impact
247 beta-lactam resistance at either acidic or neutral pH. These data are consistent with what has
248 been observed in *S.* Typhimurium in which loss of its PBP3 paralog, $PBP3_{SAL}$sensitizes cells to beta-
249 lactams targeting division[29]. In *K. pneumoniae* loss of $PBP3_{PARA}$ at low pH sensitized cells to not only
250 PBP3 inhibitors, but also to a Cephalosporin targeting class A PBPs and the penicillin, Ampicillin
251 (Figure 4 A&B). While loss of $PBP3_{PARA}$ generally sensitized *K. pneumoniae* to beta-lactams under
252 acidic conditions, it increased resistance to compounds targeting PBP2 at pH 4.8 up to 12- to 16-
253 fold (Figure 5A). This increase in resistance in $PBP3_{PARA}$ deficient cells was eliminated in a double
254 mutant lacking both $PBP3_{PARA}$ and $PBP2_{PARA}$ (Δ*ftsI2* Δ*mrdA2*). Under acidic conditions the double
255 class B paralog mutant exhibited WT-level MICs when challenged with Meropenem or Doripenem
256 (Figure 5).

257 It is unclear why the loss of $PBP3_{PARA}$ renders cells resistant to PBP2-targeting compounds.
258 Morphological data of WT *K. pneumoniae* challenged with Meropenem at low pH reveals hybrid
259 morphologies, with cells displaying signatures of both divisome and elongasome inhibition. Cells
260 first undergo lengthening and then display large, rounded septal bulges (Fig 5C). These results
261 could reflect altered target binding by Meropenem at low pH, where PBP3/$PBP3_{PARA}$ are also
262 inhibited along with PBP2/$PBP2_{PARA}$. Alternatively, physical interactions between class B PBPs
263 within the elongasome and divisome have been reported in *E. coli*[30], and data suggests that the
264 protein components of the PG synthesis complexes in *Salmonella* vary depending on whether the
265 canonical or paralogous class B PBP is present in the complex[20,31]. Alterations to interactions
266 between class B PBP paralogs and other cell wall synthesis proteins due to beta-lactam binding or
267 in the class B PBP paralog mutant backgrounds could influence morphology and antibiotic
268 resistance. Additional work is needed to fully understand the complex role that the class B PBP
269 paralogs play in resistance to PBP2-targeting beta-lactams.

270 **$PBP3_{PARA}$ is critical for *K. pneumoniae* division at low pH**

271 Our data suggest that $PBP3_{PARA}$ is the major transpeptidase supporting cross wall synthesis at low
272 pH. Loss of $PBP3_{PARA}$ did not impact cell length at neutral pH but impaired division at low pH
273 resulting in filamentous cells. However, these acid-cultured $PBP3_{PARA}$-deficient filamentous cells
274 were able to resume division and return to WT-lengths if they were transitioned to neutral pH
275 (Sfig3), suggesting that the canonical PBP3 is unable to fully compensate for the loss of $PBP3_{PARA}$ at
276 low pH. We attempted to disrupt the canonical PBP3 under acidic culture conditions where
277 $PBP3_{PARA}$ is likely the dominate division-specific transpeptidase; however, despite multiple
278 attempts, we were unsuccessful. Moreover, a small percentage of Δ*ftsI2* cells maintained WT-
279 lengths at low pH, suggesting that the canonical PBP3 retains limited, but critical activity at low pH
280 (Sfig2). These data differ from *Salmonella* where the canonical PBP3 and PBP3 paralog $PBP3_{SAL}$ are
281 individually dispensable at low pH. The canonical PBP3 is capable of supporting growth at both low
282 and neutral pH, but $PBP3_{SAL}$ is unable to support division at neutral pH[19]. Our results support a
283 model in which *K. pneumoniae* PBP3 functions optimally at neutral pH while $PBP3_{PARA}$ functions
284 predominately at acidic pH, with both working together to ensure that division remains robust
285 across pH conditions.

286 **Expansion and pH specialization of *K. pneumoniae* cell wall synthesis enzymes provide novel**
287 **therapeutic targets**

288 Identification of paralogous class B PBPs has thus far only been described in pathogens [18–20,32], but
289 the role of these paralogous cell wall synthesis proteins in pathogen physiology remains largely
290 uncharacterized. In *Salmonella,* the acid-responsiveness of class B PBP paralogs raised
291 speculation that they could be critical to support bacterial survival during intracellular growth
292 within acidified host immune cells. However, loss of the class B PBP paralogs did not impair
293 replication within macrophages or attenuate virulence in a mouse infection model[19].

294 In *Klebsiella pneumoniae* our data suggests that class B PBP paralogs are part of a general strategy
295 of functional redundancy to preserve critical enzymatic activity across a wide range of
296 environmental conditions. Colonization of a host exposes a bacterial pathogen to a wide range of
297 pH conditions[33–35] . We demonstrate that the acidification of growth medium to physiologically-
298 relevant levels is sufficient to increase resistance to beta-lactams. The class B PBP paralogs
299 modulate that resistance in part, suggesting that these pathogen-specific proteins may provide

300 novel therapeutic targets. We propose that future screens for new antimicrobial targets factor
301 environmental pH as a variable in order to identify novel compounds that can bind to acid-
302 responsive targets such as the Class B PBP paralogs. Altogether, our results highlight the need to
303 evaluate pathogen physiology in diverse environments beyond the standard laboratory conditions.

304 **Acknowledgements**

305 We are indebted to members of the Levin lab for their feedback and discussion regarding this
306 study. We alsothank Kyra Raines and Dr. Sarah Anderson for critical reading of this manuscript.
307 This work has been funded by the NIH through an G35-GM127331 award to P.A.L.

308 **Contributions**

309 S.B.: Conceptualization, Investigation, Formal analysis, Methodology, Visualization, Writing-
310 original draft, Writing – review and editing.

311 P.A.L.: Conceptualization, Funding acquisition, Resources, Supervision, Writing – review and
312 editing.

313 **Data availability**

314 All raw and processed data required to evaluate the conclusions of this study are included in the
315 text or supplemental data. The RNA sequencing data for gene expression studies at acidic and
316 neutral pH have been deposited in the NCBI GEO repository: GSE291667.

317 **Methods**

318 **Bacterial strains, growth conditions, and antibiotics.**

319 Bacterial strains and plasmids used in this study are listed in Supplementary table 1 and
320 Supplementary table 2. Strains were routinely cultured in Lysogeny Broth (LB – 1% Tryptone, 0.5%
321 Yeast extract, and 1% NaCl) in large glass tubes at 37 °C with 200 RPM aeration. The pH of LB was
322 adjusted with 1:10 MMT buffer (1:2:2 molar ratio of D/L-malic acid, MES, and Tris base). Where
323 indicated cultures were supplemented with Kanamycin (50 µg/mL), Spectinomycin (100 µg/mL),
324 Chloramphenicol (50 µg/mL), or IPTG (0.1 mM) . The pRDC3 plasmid (p15A ori, SpecR, Plac) was a
325 gift from Fabrizio Arigoni. Plasmid pSDB8 was generated from pRDC3 using the IVA cloning method
326 to insert *ftsI2* under control of the Plac promoter[36]. Primers were acquired from Integrated DNA
327 Technologies (Coralville, IA) and sequences used are listed in Supp Table 3. Chemically competent

328 *E. coli* TOP10 were used to assemble vectors via IVA. Plasmid sequence was confirmed via whole
329 plasmid sequencing at Plasmidsaurus prior to transformation into *K. pneumoniae* strains.

330 For growth studies, cultures were started LB supplemented with MMT buffer to the indicated pH
331 and grown in large glass tubes at 37 °C with 200 RPM aeration. Cultures were harvested once they
332 reached mid-exponential phase (OD_{600} =0.2-0.6), concentrated to an OD_{600} =1.0, and serially
333 diluted 10-fold. 1.5 µL of the 10^{-5} dilution was used to inoculate wells of sterile 96-well plates
334 containing 150 µL of LB + MMT at indicated pH. The plate was covered with a Breathe-Easy strip
335 (Diversified Biosciences) and growth was monitored in a BioTek Synergy H1 plate reader with the
336 following settings: 37 °C, continuous double orbital shaking at 282 cpm, with OD_{600} readings taken
337 every 10 minutes.

338 For *ftsI2* cell size complementation studies, un-induced overnight cultures of strains carrying either
339 pRDC3 (Empty vector, EV) or pSDB8 were back-diluted 1:500 into 3 mL of fresh LB buffered to
340 either pH 4.8 or pH 6.8 containing Spectinomycin (100 µg/mL). Cultures were grown at 37 °C with
341 200 RPM aeration for 1.5 hrs. Expression of *ftsI2* was induced with the addition of 0.1 mM IPTG and
342 cultures were allowed to continue growing until early exponential phase (OD_{600} = 0.1-0.3) was
343 reached (~40-90 additional minutes). Cultures were back-diluted into fresh buffered media
344 containing Spectinomycin (100 µg/mL) and 0.1 mM IPTG to an OD_{600} ~= 0.005. Growth was
345 monitored every 30 minutes, and cells were harvested when cultures reached early exponential
346 phase (OD_{600} = 0.1-0.3). Cells were spotted onto media pads (LB + MMT (pH 4.8 or 6.8) +
347 Spectinomycin (100 µg/mL) + 0.1 mM IPTG + 1% agarose and imaged live with phase microscopy.

348 The following antibiotics used for antibiotic susceptibility screenings. Ampicillin sodium salt,
349 Aztreonam, Cephalexin hydrate, Cefsulodin sodium salt hydrate, Meropenem Trihydrate, and
350 Piperacillin sodium salt were obtained from Sigma Adrich (St. Louis, MO). Carbenicillin sodium salt
351 was from EMD Millipore (now Millipore Sigma, Germany). Doripenem was obtained from Cayman
352 Chemicals (Ann Arbor, MI).

353 **Genetic manipulation:** Gene disruptions were carried out in the *K. pneumoniae* TOP52
354 background using a Lambda Red vector modified to carry a Spectinomycin resistance cassette as
355 described previously [37,38]. Briefly, DreamTaq Polymerase (Thermo Scientific) was used to PCR
356 amplify the Kanamycin resistance cassette from the template plasmid pKD4 with primers
357 containing 40-60 bp of homology to the chromosomal targets. Primers were designed to leave the

358 start and stop codons of the targeted gene intact. Linear PCR products were purified using a
359 Purelink PCR purification kit (Invitrogen), and electroporated into *K. pneumoniae* cells expressing
360 the Lambda Red recombinase system from the pKD46S plasmid. Electroporated cells were
361 recovered in SOC (Lloyd's recipe) for 4-8hrs at 30°C. Deletion mutants were selected for by plating
362 transformation culture onto LB agar plates containing Kanamycin (50 µg/mL) and incubated at
363 37°C. Mutants were confirmed by colony PCR and sequencing as necessary. For marker-less
364 deletions, cells were transformed with pCP20 at 30°C in LB + Chloramphenicol (50 µg/mL) to
365 express the FLP to excise the FRT-flanked Kanamycin cassette. After excision, cells were cultured
366 at 42°C to promote loss of pCP20. Kanamycin and Chloramphenicol sensitivity was confirmed for
367 strains prior to use.

368 **RNA sequencing**: *K. pneumoniae* TOP52 or *E. coli* MG1655 was cultured overnight in LB buffered
369 to either pH 4.8 or 6.8 with MMT buffer. Overnight cultures were back diluted 1:100 into fresh media
370 and cultured at 37°C with 200 RPM aeration until cultures reached early exponential phase (OD_{600}
371 =~0.2). ~ 9.6 x 10^8 cells were transferred to 15 mL conical Falcon tubes and pelleted by
372 centrifugation at 4°C (4,000 RPM for 10 mins). The supernatant was discarded, cell pellets were
373 resuspended in 350 uL of RNAwiz, and the RNA was extracted following the protocol for the
374 Ribopure-Bacteria RNA extraction kit [Invitrogen]. RNA was eluted in 50 uL of elution solution.
375 Purified RNA was subjected to a DNase I treatment to remove any contaminating chromosomal
376 DNA. RNA sequencing and differential gene expression analysis was performed by MiGS. Quality
377 control and adapter trimming of reads was performed with bcl2fastq. Read mapping was
378 performed with HISAT2, and read quantification was performed using Subread's featureCounts.
379 Read counts were normalized in R using edgeR's Trimmed Mean of M values (TMM) algorithm, and
380 subsequent values were converted to counts per million (CPM). Differential expression analysis
381 was performed using edgeR's Quasi-Linear F-Test (qlfTest) functionality against treatment groups,
382 and DEGs were considered as those with $|logFC| > 1$ and $p < .05$. Three biological replicates were
383 submitted per pH condition.

384 **Antibiotic susceptibility testing.** Cells were cultured from a single colony in LB at the indicated
385 pH to exponential phase (OD_{600} =~0.2-0.6) at 37 °C with 200 RPM aeration. Harvested cells were
386 concentrated to an OD_{600} =1 and serially diluted 10-fold. 1.5 µL of the 10^{-2} dilution was used to seed
387 wells containing 150 µL of LB broth + MMT (matching pH) in sterile 96-well microtiter plates
388 containing a range of two-fold dilutions of beta-lactam antibiotics. Plates were sealed with a

389 Breathe-Easy strip (Diversified Biotech) and incubated for 20 hours at 37°C with 200 RPM aeration.
390 The minimal inhibitory concentration (MIC) was determined by visual inspection and reflects the
391 lowest drug concentration that completely inhibited bacterial growth.

392 **Terminal morphology Assessment.** At the end of 20 hours for antibiotic susceptibility tests, cells
393 were taken from wells following growth at either neutral or acidic pH with the indicated antibiotic
394 concentrations. 5 µL of cells were spotted onto LB + 1% agarose and imaged by phase contrast
395 microscopy.

396 **Microscopy, cell size analysis, and time-lapse Imaging.** All phase contrast and fluorescence
397 images were acquired on either a Nikon Ti-E inverted microscope or a Ti2-E inverted microscope
398 (Nikon Instruments). The Ti-E is equipped with a 100X Plan Apo oil objective (N.A. = 1.45 Ph3
399 objective, X-Cite 120 LED light source (Lumen Dynamics) and an OrcaERG CCD camera
400 (Hammamatsu Photonics, Bridgewater, N.J.) Filter cubes were purchased from Chroma
401 Technology Corporation. The Ti2-E inverted microscope is equipped with a 100X Plan Apo oil
402 objective (N.A. = 1.45, Ph3 objective, Lumencor Sola LED light engine (Lumencore), and an orca-
403 Fusion sCMOS camera (Hammamatsu Photonics). Filter cubes were purchased from Chroma
404 Technology Corporation. Both microscopes have an enclosed temperature-controlled enclosure to
405 pre-heat the objective to 37 °C (OXO enclosure) prior to experiments. Nikon Elements software was
406 used for image capture, and analysis was performed using the MicrobeJ plug-in in ImageJ.

407 For cell size analysis, cells were grown from a single colony in LB with MMT buffer at indicated pH
408 at 37 °C and 200 RPM aeration to exponential phase (OD_{600} = 0.2-0.4) and back-diluted to an OD_{600}
409 = 0.005 into 7 mL of pre-warmed LB + MTT (same pH). Growth was monitored via optical density,
410 and when cultures reached early exponential phase (OD_{600} =0.1- 0.2) cells were harvested. 5 µL of
411 cells were spotted onto LB + MTT (same pH)+ 1% agarose pads and imaged by phase contrast
412 microscopy. Cell morphology and size dimensions were determined using the MicrobeJ[39] plug-in
413 for ImageJ.

414 For time-lapse imaging, cultures were grown from a single colony in LB with MMT buffer at
415 indicated pH at 37 °C and 200 RPM aeration to exponential phase (OD_{600} = 0.1-0.4). 5 µL of cells
416 were spotted onto LB + MTT (same pH)+ 1% agarose pads that contain antibiotics at indicated
417 concentrations and 1.5 µM propidium iodide (PI) for monitoring loss of membrane integrity. Phase
418 images were obtained every 2 minutes, and fluorescent images were collected every 10 minutes

419 (100 mS exposure/10% intensity). For each experiment a total of 2-5 different XY coordinates were
420 monitored throughout the duration of the experiment. Quantification of PI^+ cells was done using
421 the MicrobeJ[39] plug-in for ImageJ. Briefly the number of cells in the phase image and the number of
422 corresponding fluorescent cells were quantified. Data was reported as either percentage of PI^+
423 cells (number of PI^+ cells/total number of cells *100) or percent alive (number of cells-PI^+ cells/total
424 number of cells*100).

425 **Bibliography**

426 1. Egan, A. J. F., Errington, J. & Vollmer, W. Regulation of peptidoglycan synthesis and
427 remodelling. *Nature Reviews Microbiology 2020 18:8* **18**, 446–460 (2020).
428 2. Pazos, M., Peters, K. & Vollmer, W. Robust peptidoglycan growth by dynamic and variable
429 multi-protein complexes. *Current Opinion in Microbiology* **36**, 55–61 (2017).
430 3. Kato, J., Suzuki, H. & Hirota, Y. Dispensability of either penicillin-binding protein -1a or -1b
431 involved in the essential process for cell elongation in Escherichia coli. *Molec. Gen. Genet.*
432 **200**, 272–277 (1985).
433 4. Suzuki, H., Nishimura, Y. & Hirota, Y. On the process of cellular division in Escherichia coli: a
434 series of mutants of E. coli altered in the penicillin-binding proteins. *Proceedings of the*
435 *National Academy of Sciences* **75**, 664–668 (1978).
436 5. Yousif, S. Y., Broome-Smith, J. K. & Spratt, B. G. Lysis of Escherichia coli by beta-lactam
437 antibiotics: deletion analysis of the role of penicillin-binding proteins 1A and 1B. *J Gen*
438 *Microbiol* **131**, 2839–2845 (1985).
439 6. Schiffer, G. & Höltje, J.-V. Cloning and Characterization of PBP 1C, a Third Member of the
440 Multimodular Class A Penicillin-binding Proteins of *Escherichia coli* *. *Journal of Biological*
441 *Chemistry* **274**, 32031–32039 (1999).
442 7. Bush, K. & Bradford, P. A. β-Lactams and β-Lactamase Inhibitors: An Overview. *Cold Spring*
443 *Harbor Perspectives in Medicine* **6**, a025247 (2016).

8. Mueller, E. A., Egan, A. J. F., Breukink, E., Vollmer, W. & Levin, P. A. Plasticity of Escherichia coli cell wall metabolism promotes fitness and antibiotic resistance across environmental conditions. *eLife* **8**, (2019).
9. Centers for Disease Control and Prevention (U.S.). *Antibiotic Resistance Threats in the United States, 2019*. https://stacks.cdc.gov/view/cdc/82532 (2019) doi:10.15620/cdc:82532.
10. Murray, C. J. *et al.* Global burden of bacterial antimicrobial resistance in 2019: a systematic analysis. *The Lancet* **399**, 629–655 (2022).
11. Johnson, J. G., Spurbeck, R. R., Sandhu, S. K. & Matson, J. S. Genome sequence of Klebsiella pneumoniae urinary tract isolate Top52. *Genome Announcements* **2**, 668–682 (2014).
12. Sutaria, D. S. *et al.* First penicillin-binding protein occupancy patterns of - Lactams and - lactamase inhibitors in klebsiella pneumoniae. *Antimicrobial Agents and Chemotherapy* **62**, (2018).
13. Bush, K. & Jacoby, G. A. Updated functional classification of β-lactamases. *Antimicrobial Agents and Chemotherapy* **54**, 969–976 (2010).
14. Kannan, G. *et al.* Rapid acid treatment of Escherichia coli: Transcriptomic response and recovery. *BMC Microbiology* **8**, 37 (2008).
15. Maurer, L. M., Yohannes, E., Bondurant, S. S., Radmacher, M. & Slonczewski, J. L. pH Regulates Genes for Flagellar Motility, Catabolism, and Oxidative Stress in Escherichia coli K-12. *Journal of Bacteriology* **187**, 304–319 (2005).
16. Choi, U., Park, S. H., Lee, H. B., Son, J. E. & Lee, C.-R. Coordinated and Distinct Roles of Peptidoglycan Carboxypeptidases DacC and DacA in Cell Growth and Shape Maintenance under Stress Conditions. *Microbiology Spectrum* **11**, e00014-23 (2023).
17. Peters, K. *et al.* The redundancy of peptidoglycan carboxypeptidases ensures robust cell shape maintenance in Escherichia coli. *mBio* **7**, (2016).

468 18. Identification of a penicillin-binding protein 3 homolog, PBP3x, in Pseudomonas aeruginosa:
469 gene cloning and growth phase-dependent expression.
470 https://journals.asm.org/doi/epdf/10.1128/jb.179.5.1490-1496.1997
471 doi:10.1128/jb.179.5.1490-1496.1997.
472 19. Castanheira, S. *et al.* A Specialized Peptidoglycan Synthase Promotes Salmonella Cell Division
473 inside Host Cells. *mBio* **8**, 10.1128/mbio.01685-17 (2017).
474 20. Castanheira, S. & García-del Portillo, F. Evidence of two differentially regulated elongasomes in
475 Salmonella. *Commun Biol* **6**, 923 (2023).
476 21. Sub-Inhibitory Cefsulodin Sensitization of E. coli to β-lactams Is Mediated by PBP1b Inhibition |
477 PLOS One. https://journals.plos.org/plosone/article?id=10.1371/journal.pone.0048598.
478 22. Ramachandran, V. *et al.* Screen for Inhibitors of the Coupled Transglycosylase-Transpeptidase
479 of Peptidoglycan Biosynthesis in Escherichia coli. *Antimicrobial Agents and Chemotherapy* **50**,
480 1425–1432 (2006).
481 23. Curtis, N. A. C., Eisenstadt, R. L., Turner, K. A. & White, A. J. Inhibition of penicillin-binding
482 protein 3 of Escherichia coli K-12. Effects upon growth, viability and outer membrane barrier
483 function. *Journal of Antimicrobial Chemotherapy* **16**, 287–296 (1985).
484 24. Buijs, J., Dofferhoff, A. S. M., Mouton, J. W., Wagenvoort, J. H. T. & van der Meer, J. W. M.
485 Concentration-dependency of β-lactam-induced filament formation in Gram-negative
486 bacteria. *Clinical Microbiology and Infection* **14**, 344–349 (2008).
487 25. Paradis-Bleau, C. *et al.* Lipoprotein Cofactors Located in the Outer Membrane Activate
488 Bacterial Cell Wall Polymerases. *Cell* **143**, 1110–1120 (2010).
489 26. Nichols, R. J. *et al.* Phenotypic Landscape of a Bacterial Cell. *Cell* **144**, 143–156 (2011).

490 27. Boes, A., Olatunji, S., Breukink, E. & Terrak, M. Regulation of the Peptidoglycan Polymerase
491 Activity of PBP1b by Antagonist Actions of the Core Divisome Proteins FtsBLQ and FtsN. *mBio*
492 **10**, 10.1128/mbio.01912-18 (2019).
493 28. Bertsche, U. *et al.* Interaction between two murein (peptidoglycan) synthases, PBP3 and
494 PBP1B, in Escherichia coli. *Molecular microbiology* **61**, 675–690 (2006).
495 29. Castanheira, S. *et al.* An alternative penicillin-binding protein involved in *Salmonella* relapses
496 following ceftriaxone therapy. *eBioMedicine* **55**, 102771 (2020).
497 30. van der Ploeg, R. *et al.* Colocalization and interaction between elongasome and divisome
498 during a preparative cell division phase in scherichia coli. *Molecular Microbiology* **87**, 1074–
499 1087 (2013).
500 31. Castanheira, S., López-Escarpa, D., Paradela, A. & García-del Portillo, F. In Vivo Cross-Linking
501 Sheds Light on the Salmonella Divisome in Which PBP3 and PBP3 Compete for Occupancy.
502 *Molecular Microbiology* **n/a**,.
503 32. Hardy, C. D. Essential Paralogous Proteins as Potential Antibiotic Multitargets in Escherichia
504 coli. *Microbiology Spectrum* **10**, e02043-22 (2022).
505 33. Machen, T. E. & Paradiso, A. M. Regulation of intracellular pH in the stomach. *Annu Rev Physiol*
506 **49**, 19–33 (1987).
507 34. Fallingborg, J. Intraluminal pH of the human gastrointestinal tract. *Dan Med Bull* **46**, 183–196
508 (1999).
509 35. O'Hanlon, D. E., Come, R. A. & Moench, T. R. Vaginal pH measured in vivo: lactobacilli
510 determine pH and lactic acid concentration. *BMC Microbiol* **19**, 13 (2019).
511 36. García-nafría, J., Watson, J. F. & Greger, I. H. OPEN IVA cloning : A single-tube universal cloning
512 system exploiting bacterial In Vivo Assembly. *Nature Publishing Group* 1–12 (2016)
513 doi:10.1038/srep27459.

514 37. Bachman, M. A. *et al*. Genome-wide identification of Klebsiella pneumoniae fitness genes
515 during lung infection. *mBio* **6**, (2015).
516 38. Datsenko, K. A. & Wanner, B. L. One-step inactivation of chromosomal genes in Escherichia
517 coli K-12 using PCR products. *Proceedings of the National Academy of Sciences* **97**, 6640–6645
518 (2000).
519 39. Ducret, A., Quardokus, E. M. & Brun, Y. V. MicrobeJ, a tool for high throughput bacterial cell
520 detection and quantitative analysis. *Nature Microbiology* **1**, 1–7 (2016).

521

522 **Figure Legends**

523 **Fig 1. *Klebsiella pneumoniae* exhibits acid-dependent resistance to Beta-lactams that is**
524 **independent of Beta-lactamase expression.**

525 (A) Heatmap displaying the fold-change in minimal inhibitory change (MIC) for *K. pneumoniae*
526 TOP52 at indicated pH relative to neutral pH. Each cell represents the median fold-change value
527 from a minimum of three biological replicates performed in LB buffered to indicated pH with MMT
528 buffer. Specific Beta-lactam antibiotics along with their preferential PBP target are indicated on the
529 Y-axis. NS = non-specific (B) The fold-change in Meropenem (MER) or Cephalexin (CEX) MIC of *K.*
530 *pnuemoniae* strains ATCC 43816 and NHUT-K2044 grown at pH 4.8 compared to growth at pH 6.8.
531 Bars represent mean and error bars denote standard deviation. C-D) Representative micrographs
532 of terminal morphologies of *K. pneumoniae* TOP52 following growth for 20 hours in LB (pH 4.8 or
533 6.8) and treated with Meropenem (C) or Cephalexin (D) at indicated concentrations. Scale bar = 2
534 µm.

535 **Fig 2. Loss of either PBP1b or PBP3$_{PARA}$ results in differential impacts to beta-lactam**
536 **resistance at low pH.** (A-D) Fold change in MICs at pH 4.8 relative to pH 6.8 shown for generalist
537 (A), class A-targeting (B), PBP2-targeting (C), and PBP3-targeting (D) beta-lactams. Data are
538 graphed as median values with range. (E) Micrographs from time-lapse microscopy of WT (top) or
539 Δ*mrcB* (bottom) growing in the presence of CEX at low pH. Microscopy pads comprised of LB
540 buffered with MMT to pH 4.8 + 15.6 µg/mL CEX + 1.5 µM propidium iodide + 1% agarose. The CEX
541 concentration reflects the 1X MIC for the Δ*mrcB* mutant and 0.06X MIC for the WT strain.

542 **Fig 3. *Klebsiella pneumoniae* possesses acid-responsive paralogous copies of the Class B**
543 **PBPs.** (A) Genomic regions containing the canonical PBP2, encoded by *mrdA*, and the paralogous
544 gene *mrdA2,* which encodes $PBP2_{PARA}$ (B) Genomic regions containing the canonical PBP3,
545 encoded by *ftsI,* and the paralogous gene *ftsI2,* which encodes $PBP3_{PARA}$. (C & D) Domain
546 conservation between canonical and paralogous copies of PBP2 (C) and PBP3 (D). Domains are
547 denoted as follows: Transmembrane (TM), Lipoprotein lipid attachment site (LP, PS51257) PBP-
548 dimer (Pfam: PF03717), Transpeptidase domain (Pfam: PF00905). Location of motifs that are
549 critical for enzyme catalysis are highlighted in purple.

550 **Fig 4. Loss of $PBP3_{PARA}$ impairs division at low pH.** (A) Representative micrographs of indicated
551 strains following growth in LB buffered to pH 4.8 (top panels) or growth in LB buffered to pH 6.8
552 (bottom panels). For complementation studies with either empty vector (EV) or p*ftsI2,* the media
553 was supplemented with 0.1 mM IPTG. Scale bar = 10 uM. (B-C) Quantification of cell length in (B).
554 Each data point represents the mean of a biological replicate (>50 cells analyzed for each
555 replicate). The bar represents the mean of three biological replicates, and the error bars represent
556 the standard error of the mean. Statistical significance was determined by a one-way ANOVA with
557 Tukey's correction for multiple comparisons with asterisks denoting significance as follows:** =
558 $p<0.005$, * = $p<0.5$.

559 **Fig 5. Loss of either PBP1b or $PBP3_{PARA}$ results in differential impacts to Beta-lactam**
560 **resistance at low pH.** (A-D) Fold change in MICs at pH 4.8 relative to pH 6.8 shown for generalist
561 (A), class A-targeting (B),PBP2-targeting (C), and PBP3-targeting Beta-lactams. For comparison,
562 data for MER and CEX are re-graphed from Fig 4. Data are presented as median values with range.
563 (E) Micrographs from time-lapse microscopy of WT, Δ*ftsI2,* Δ*mrdA2,* and Δ*mrdA2* Δ*ftsI2* growing in
564 the presence of MER at low pH. Microscopy pads comprised of LB buffered with MMT to pH 4.8 +
565 0.2 µg/mL MER + 1.5 µM propidium iodide + 1% agarose. The MER concentration reflects 1X MIC for
566 WT, ~0.25X MIC for Δ*ftsI2,* ~2X MIC for Δ*mrdA2,* and ~0.5X MIC for Δ*mrdA2* Δ*ftsI2.*

567

Fig 1

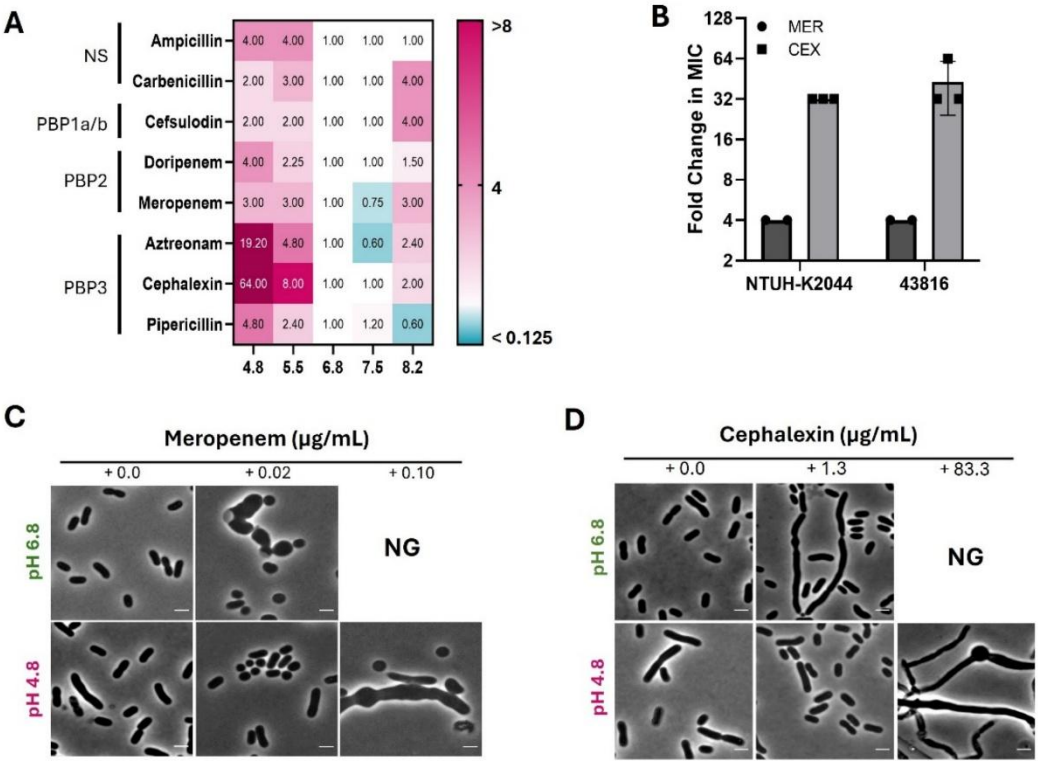
A
NS
Ampicillin
Carbenicillin
PBP1a/b
Cefsulodin
PBP2
Doripenem
Meropenem
PBP3
Aztreonam
Cephalexin
Pipericillin
4.00 4.00 1.00 1.00 1.00
2.00 3.00 1.00 1.00 4.00
2.00 2.00 1.00 1.00 4.00
4.00 2.25 1.00 1.00 1.50
3.00 3.00 1.00 0.75 3.00
19.20 4.80 1.00 0.60 2.40
64.00 8.00 1.00 1.00 2.00
4.80 2.40 1.00 1.20 0.60
4.8 5.5 6.8 7.5 8.2
>8
4
< 0.125
B
MER
CEX
Fold Change in MIC
128
64
32
16
8
4
2
NTUH-K2044
43816
C
Meropenem (μg/mL)
+ 0.0
+ 0.02
+ 0.10
pH 6.8
pH 4.8
NG
D
Cephalexin (μg/mL)
+ 0.0
+ 1.3
+ 83.3
pH 6.8
pH 4.8
NG

568

569

Fig 2

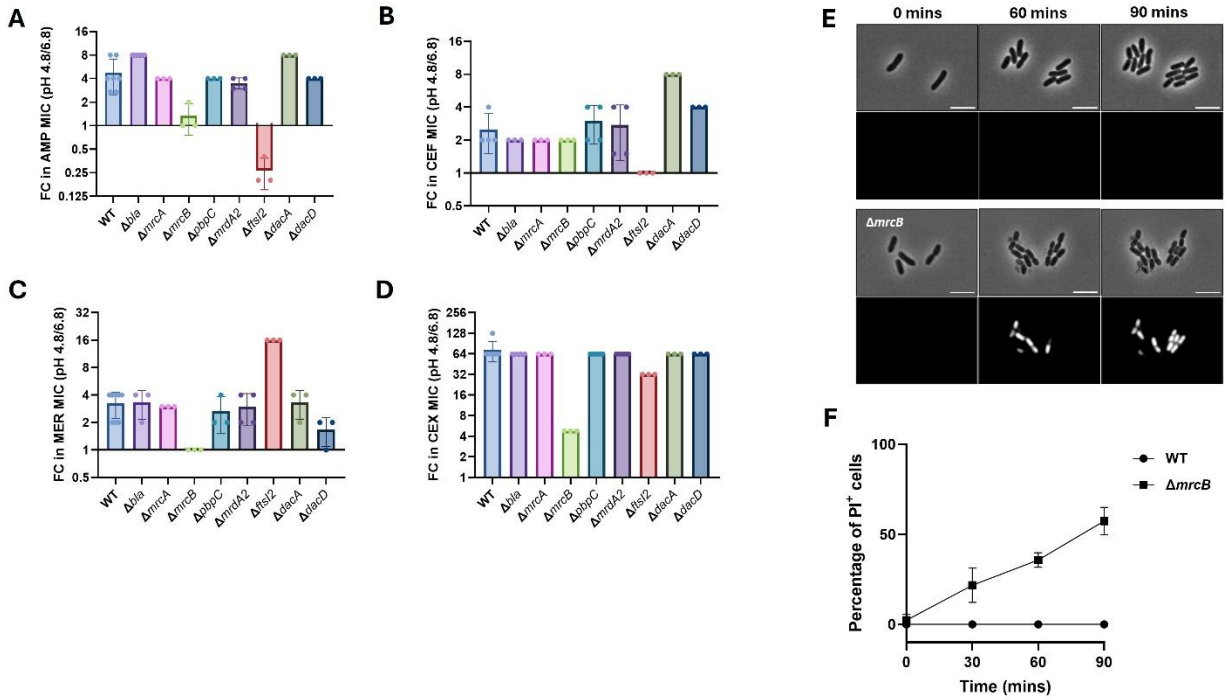
A
FC in AMP MIC (pH 4.8/6.8)
B
FC in CEF MIC (pH 4.8/6.8)
C
FC in MER MIC (pH 4.8/6.8)
D
FC in CEX MIC (pH 4.8/6.8)
WT
Δbla
ΔmrcA
ΔmrcB
ΔpbpC
ΔmrdA2
Δftsl2
ΔdacA
ΔdacD
E
0 mins
60 mins
90 mins
ΔmrcB
F
Percentage of PI+ cells
Time (mins)
WT
ΔmrcB

570

571

Fig 3

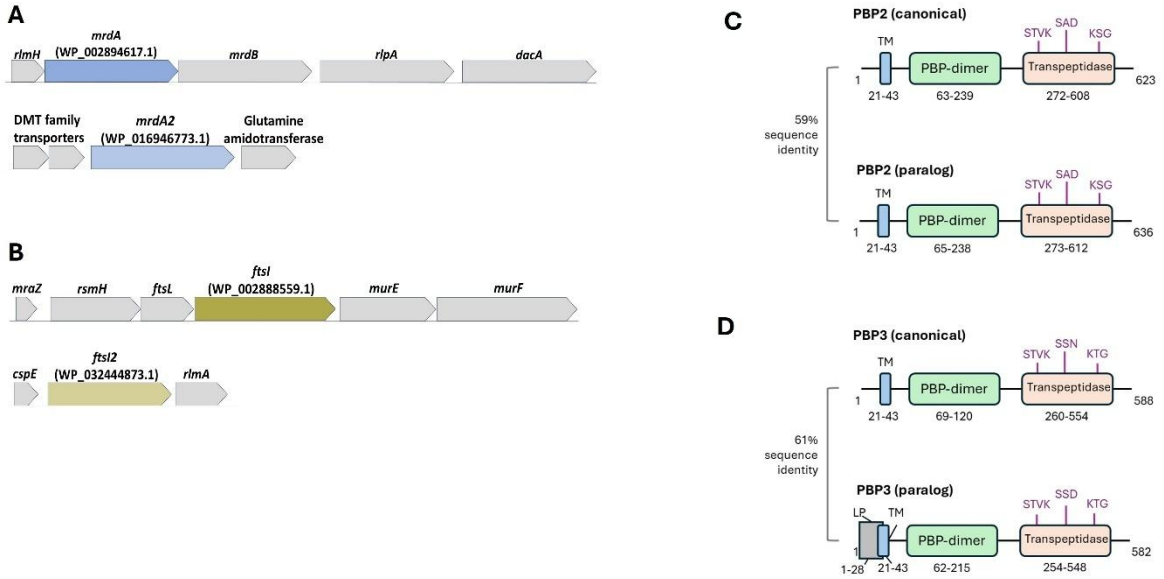

572

573

Fig 4

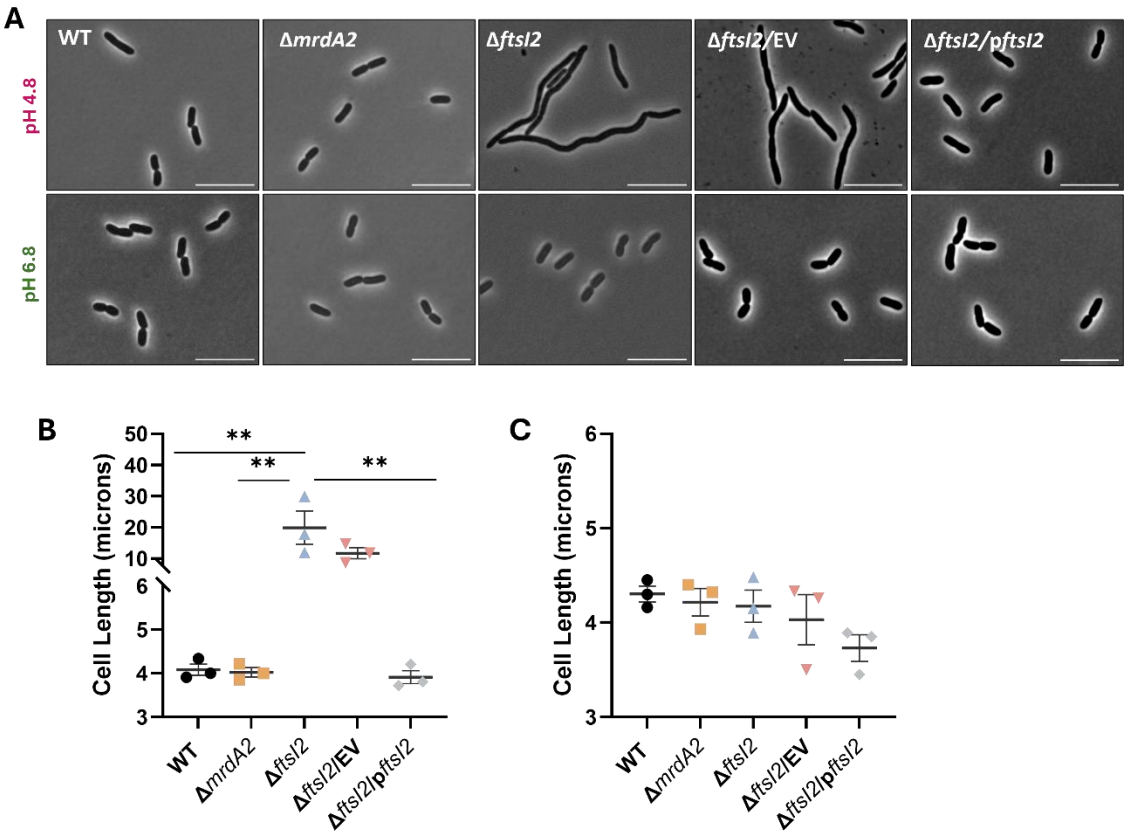
A
WT
ΔmrdA2
ΔftsI2
ΔftsI2/EV
ΔftsI2/pftsI2
pH 4.8
pH 6.8
B
Cell Length (microns)
50
40
30
20
10
6
5
4
3
**
**
**
WT
ΔmrdA2
ΔftsI2
ΔftsI2/EV
ΔftsI2/pftsI2
C
Cell Length (microns)
6
5
4
3
WT
ΔmrdA2
ΔftsI2
ΔftsI2/EV
ΔftsI2/pftsI2

574

575

576

Fig 5

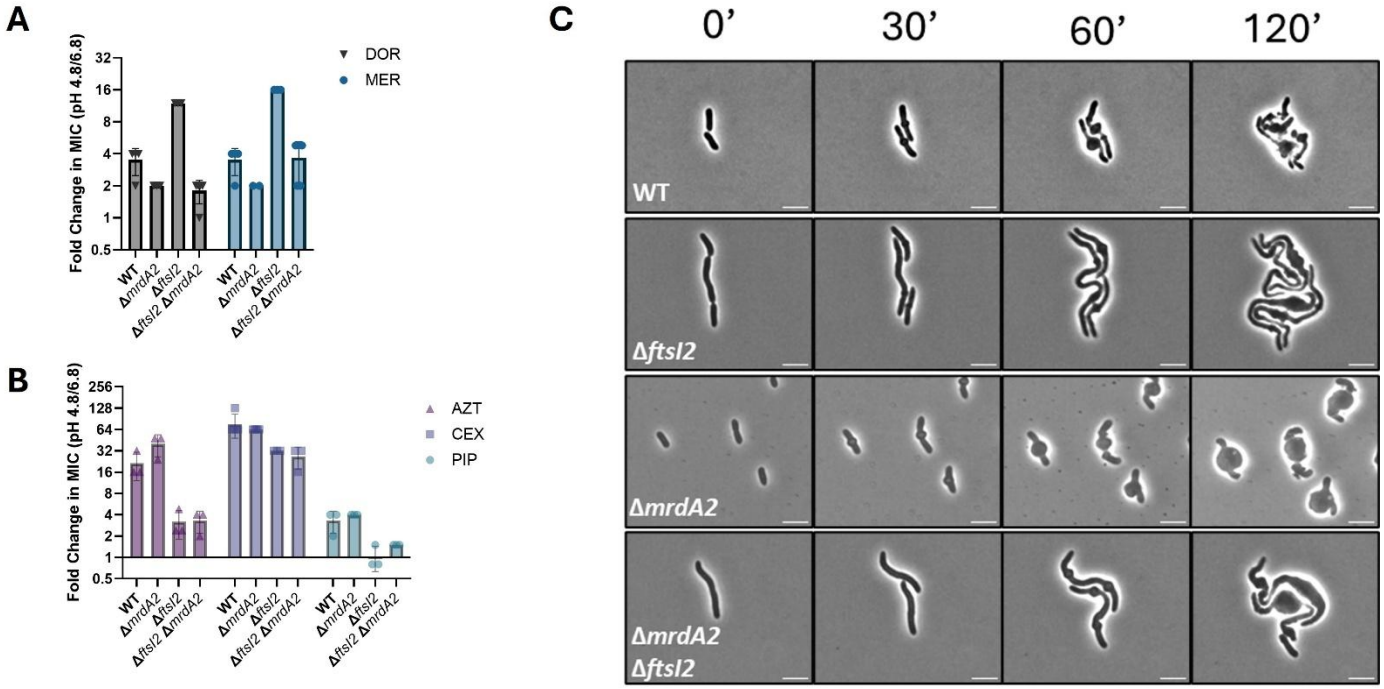
A
Fold Change in MIC (pH 4.8/6.8)
32
16
8
4
2
1
0.5
DOR
MER
WT
ΔmrdA2
ΔftsI2
ΔftsI2 ΔmrdA2
B
256
128
AZT
CEX
PIP
C
0'
30'
60'
120'
WT
ΔftsI2
ΔmrdA2
ΔmrdA2
ΔftsI2

577

578 **Table 1. Transcriptional response to pH of key beta-lactam targets in *K. pneumoniae* and *E.***
579 ***coli***

	Gene	Enzyme Encoded	Description	log_2FC (pH 4.8/6.8)
K. pneumoniae				
D1637_RS05825	*mrcA*	PBP1a	bifunctional glycosyl transferase/transpeptidase	0.60
D1637_RS12385	*mrcB*	PBP1b	bifunctional glycosyl transferase/transpeptidase	-0.39
D1637_RS01040	*pbpC*	PBP1c	peptidoglycan glycosyltransferase	-1.61
D1637_RS15400	*mrdA*	PBP2	canonical peptidoglycan DD-transpeptidase	0.84
D1637_RS12000	*ftsI*	PBP3	canonical peptidoglycan DD-transpeptidase	0.23
D1637_RS21590	*mrdA2*	$PBP2_{para}$	paralogous peptidoglycan DD-transpeptidase	3.41
D1637_RS24275	*ftsI2*	$PBP3_{para}$	paralogous peptidoglycan DD-transpeptidase	3.28
D1637_RS15385	*dacA*	PBP5	D-Ala-D-Ala-carboxypeptidase	1.20
D1637_RS25010	*dacD*	PBP6b	D-Ala-D-Ala carboxypeptidase	1.63
E. coli				
b3396	*mrcA*	PBP1a	bifunctional glycosyl transferase/transpeptidase	0.36
b0149	*mrcB*	PBP1b	bifunctional glycosyl transferase/transpeptidase	-0.23
b2519	*pbpC*	PBP1c	peptidoglycan glycosyltransferase	-0.43
b0635	*mrdA*	PBP2	canonical peptidoglycan DD-transpeptidase	0.47
b0084	*ftsI*	PBP3	canonical peptidoglycan DD-transpeptidase	-0.64
b0632	*dacA*	PBP5	D-alanyl-D-alanine carboxypeptidase	0.95
b2010	*dacD*	PBP6b	D-alanyl-D-alanine carboxypeptidase	2.63

580 *****Shaded genes represent those that were differentially regulated by pH as determined by our cutoff
581 of |logFC| > 1 and $p < .05$. Blue Log_2FC values indicate that the gene was down-regulated during
582 growth at pH 4.8 versus pH 6.8. Magenta Log_2FC values indicate that the gene was up-regulated
583 during growth at pH 4.8 versus pH 6.8.